
Vortical Interactions with Interfacial Shear Layers

J.C.R. Hunt¹, I. Eames¹ and J. Westerweel²

¹ University College London, Gower Street, London WC1E 7JE, UK

² J.H. Burgers Centre, Delft University of Technology, 2628 CA Delft, The Netherlands

Physical models based on linearised calculations are developed to provide insight into some of the complex processes which occur adjacent to shearing interfaces. Specifically the case of vortices interacting with strong and weak shearing interfaces are developed. These provide a starting point to interpret previous detailed experimental and theoretical studies.

1 Introduction

We examine aspects of eddy motion that occur at the interfacial shear layers that exist between regions of turbulent and non-turbulent motion, such as the outer edge of jets and wakes. The very inhomogeneous turbulence in these interfacial regions play a critical role in many engineering and natural flows (*e.g.* [1]). With the aid of Particle Imaging Velocimetry (PIV) systems and large computers running at mega- and tera-flops speed, the flow and scalar fields in these layers can be measured and computed in sufficient detail, to test the various hypotheses and theoretical models ([2], [3], [4]). In some previous models it was assumed that the dynamics of the interface was determined by the ‘nibbling’ action of small scale turbulent eddies (*e.g.* [5]) while others were based on the ‘engulfing’ motions of large scale eddies and the ‘elastic’ dynamics of turbulence distorted by these eddies [6].

The interaction between internal turbulence and interfacial shear layers has been previously studied theoretically using linearised RDT calculations where the interface is approximately flat (*e.g.* [7]) or weakly deformed (*e.g.* [8]). To delve deeper into the physical processes, we examine the effect of impinging vortices on the distortion of shear layers. Here we consider the effect of vortices interacting with relatively strong interfaces which leads to the strengthening of the shear layer and vortices distorting a weak interfacial layer – both processes which are observed in detailed numerical and experimental studies.

2 Dynamics of Shear Interface Layers

At an interface located at $x_3 = 0$ bounding flows with mean shear (*e.g.* jets, wakes), the mean vorticity $\Omega_2 = \partial U_1 / \partial x_2$ has the form $\langle \Omega_2 \rangle = \delta(-x_3) \Delta U_1 + H(-x_3) \langle dU_1 / dx_3 \rangle_c$. The local turbulence continually enhanced by the Kelvin-Helmholtz instability of the shear layer leads to the interface moving outwards at the boundary $E_b = \langle dx_3 / dt \rangle (x_3 = 0)$ [2]. Although previous studies have suggested $\Delta U_1 = 0$ (*e.g.* [9]), where $u_0 \sim \sqrt{u_3^2}$, numerical simulations, experiments and theory indicate that at high Reynolds numbers, a vortex sheet exists where $\Delta U_1 \neq 0$. The vortex sheet acts as a barrier to velocity fluctuations relative to the sheet (ie $u_3 = 0$ at $x_3 = 0$) provided $u_0 < \Delta U_1$ through the shear sheltering mechanism [8]. When the eddies $x_3 < 0$ move with the local mean velocity they produce a weak pressure fluctuation at the interface, but their straining motion distorts the vorticity in the shear layer so that it induces an impulse that opposes that of the impinging vortex.

2.1 Vortical Interaction with a Strong Interface

We consider an idealisation of the typical flow at the edge of a turbulent shear layer where there is a relatively strong discontinuity in the conditionally averaged velocity field at the interface, *i.e.* $u_0 \ll \Delta U_1$. In the interior turbulent region ($x_3 < 0$) near the interface, the mean external velocity profile is $U_1 = \Delta U_1^{(-)}(x_3)H(-x_3) - x_3 H(-x_3) \langle dU_1 / dx_3 \rangle_c$, and the mean shear $\Omega_2^{(-)} = \partial U_1^{(-)} / \partial x_3$, is small compared to the strain rate of the turbulent eddies and $\Omega_2 \rightarrow 0$ for $|x_3| / L_x \gg 1$. Pressure fluctuations $O(u_0^2)$ affect the interface displacing it by $\sim (u_0 / \Delta U_1) L_x$ so to first order the turbulence is blocked by the shear layer, *i.e.* $u_3^{(-)} = 0$ at $x_3 = 0$.

The aim here is to calculate the mean vorticity $\Omega_2^{(-)}$ below the interface as it is perturbed during the period that a fluid element spends within an eddy near the interface. Fluid lines parallel to the x_2 -direction are stretched which produces changes to the mean vorticity field below the interface. The local value of the spanwise component of vorticity $\Omega_2^{(-)}$ is smaller than the vorticity fluctuations $\omega^{(-)}$ of the impinging turbulence. The flow generated by a largescale disturbance moving towards the interface is blocked kinematically initially generating an approximately local linear straining flow,

$$\mathbf{u}^{(-)} = ((\lambda_3 - 1)\Sigma^{(-)}x_1, \Sigma^{(-)}x_2, -\lambda_3\Sigma^{(-)}x_3), \quad (1)$$

where $\Sigma^{(-)} > 0$ and λ_3 depends on the nature of the eddy (see Fig. 1). For short time, the linearised vorticity equation for $\Omega_2^{(-)}$ is

$$\frac{d\Omega_2^{(-)}}{dt} \left(\equiv -\lambda_3 \Sigma^{(-)} x_3 \frac{d\Omega_2^{(-)}}{dx_3} \right) = \frac{\partial u_2^{(-)}}{\partial x_2} \Omega_2^{(-)} = \Sigma^{(-)} \Omega_2^{(-)}. \quad (2)$$

The results can be expressed in a Lagrangian time coordinate t or in terms of x_3 . Since for an impinging eddy $\Omega_2^{(-)} = \Omega_{20}^{(-)}$ when $|x_3| \sim L_x$ and $t = 0$, from (2),

$$\Omega_2^{(-)}(t)/\Omega_{20}^{(-)} = \exp(\Sigma^{(-)}t), \quad \text{or} \quad \Omega_2^{(-)}(x_3)/\Omega_{20}^{(-)} = (L_x/x_3)^{1/\lambda_3}. \quad (3)$$

This shows how the distortion of the mean vorticity profile depends on the form of the eddies in the external flow below the interface, as characterised by the parameter λ_3 . As the stretching by the impinging eddies increases towards the interface, the viscous diffusion of vorticity increases until it limits any further growth at the edge of the viscous internal layer at the interface where $|x_3| \sim l_v = \sqrt{\nu/\Sigma^{(-)}}$ at the sheared interface. Defining the eddy Reynolds number $Re_v = u_0 L_x/\nu$, where $u_0 \sim \Sigma^{(-)}L_x$, the maximum value of the perturbed external vorticity is $\Omega_{2max}^{(-)}/\Omega_{20}^{(-)} \sim (L_x/l_v)^{\frac{1}{2}} \sim Re_v^{\frac{1}{4}}$, for axisymmetric straining flows/vortices (where $\lambda_3 = 2$), while $\Omega_{2max}^{(-)}/\Omega_{20}^{(-)} \sim L_x/l_v \sim Re_v^{\frac{1}{2}}$, for planar straining/longitudinal vortices (where $\lambda_3 = 1$) (see Fig. 1).

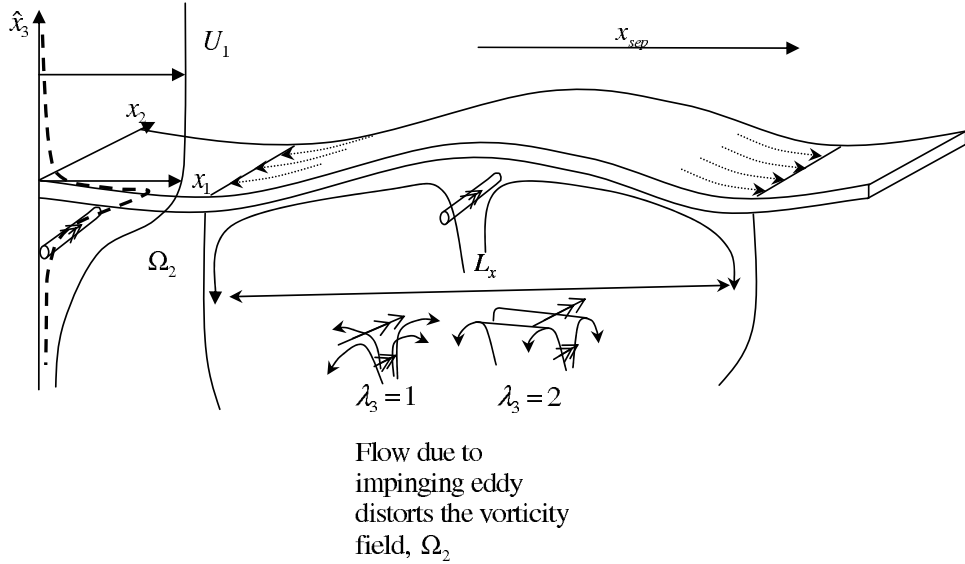


Fig. 1. Schematic showing how the distortion of vorticity by impacting planar ($\lambda_3 = 1$) and axisymmetric ($\lambda_3 = 2$) eddies on the shearing interface (located at $x_3 = 0$) serves to strengthen and maintain the interface.

In the next phase of their ‘life-cycle’, the fluid elements typically move towards the separation/stagnation regions (where $x_1 = x_{sep} \sim L_x$, see Fig. 1) where the streamlines converge along the surface before moving downwards into the turbulent region, *i.e.*

$$\mathbf{u}^{(-)} = (-\lambda_1 \Sigma^{(-)}(x_1 - x_{sep}), -\Sigma^{(-)}x_2, (1 + \lambda_1)\Sigma^{(-)}x_3), \quad (4)$$

where $\lambda_1 \sim 1$ and $\Sigma^{(-)} > 0$. Perot & Moin [10] computed the streamlines in the typically axisymmetric ‘anti-splat’ processes in their direct numerical simulations of turbulence in this kind of flow for the case of a shear-free layer. Along the surface where $x_3 \sim l_v$,

$$\frac{d\Omega_2^{(-)}}{dt} \left(= -\lambda_1 \Sigma^{(-)}(x_1 - x_{sep}) \frac{d\Omega_2^{(-)}}{dx_1} \right) = -\Omega_2^{(-)} \Sigma^{(-)}, \quad (5)$$

so that

$$\Omega_2^{(-)} / \Omega_{2max}^{(-)} = ((x_1 - x_{sep}) / L_x)^{1/\lambda_1}. \quad (6)$$

Thus although $\Omega_2^{(-)}$ tends to where the flow separates the average value of $\Omega_2^{(-)}$ along the surface is much greater than the mean value of $\Omega_2^{(-)}$, *i.e.* $\langle \Omega_{20} \rangle$, in the external turbulent region, *i.e.*

$$\langle \Omega_2^{(-)} \rangle (\tilde{x}_3 \sim -l_v) \sim \frac{1}{2} \langle \Omega_{20} \rangle / (l_v / L_x)^{1/\lambda_3}. \quad (7)$$

For highly elongated eddies, ($\lambda_3 \sim 1$) the variation of mean vorticity is given by

$$\langle \Omega_2^{(-)} \rangle \sim \Omega_{20} Re_v^{\frac{1}{2}} |x_3 / L_x|^{-1} \quad (8)$$

giving rise to an approximately logarithmic profile adjacent to the interface. While for axisymmetric vortices ($\lambda_3 \sim 2$),

$$\langle \Omega_2^{(-)} \rangle \sim \Omega_{20} Re_v^{\frac{1}{4}} |x_3 / L_x|^{-2} \quad (9)$$

a much more localised (but weaker) perturbation is created. This mechanism of inhomogeneous straining of large scale turbulence leads to a finite amplification of the mean vorticity in a layer of finite thickness.

2.2 Vortical Interaction with a Weak Interface

Observations, measurements and detailed numerical simulations of the edges of turbulent shear flows ([2], [3], [4]) show that periodically the interface forms cusps that point inwards towards the turbulent region ($x_3 < 0$). In the opposite direction smooth bulges tend to form. The local processes associated with these inward cusps are significant for the overall flow because they affect the transport of material (and scalars) across the shear layer and contribute significantly to the dissipation of energy in the turbulent region. We consider an idealised local analysis to study how the vortex sheet changes as it is entrained by the large eddy motion (see Fig. 2a). During these events the straining flow generated by the vortices or turbulence is stronger than the ambient flow, *i.e.* $u_0 \sim \Sigma^{(-)} L_x \gg \Delta U_1$ and the velocity of the large scale eddies u_0 in

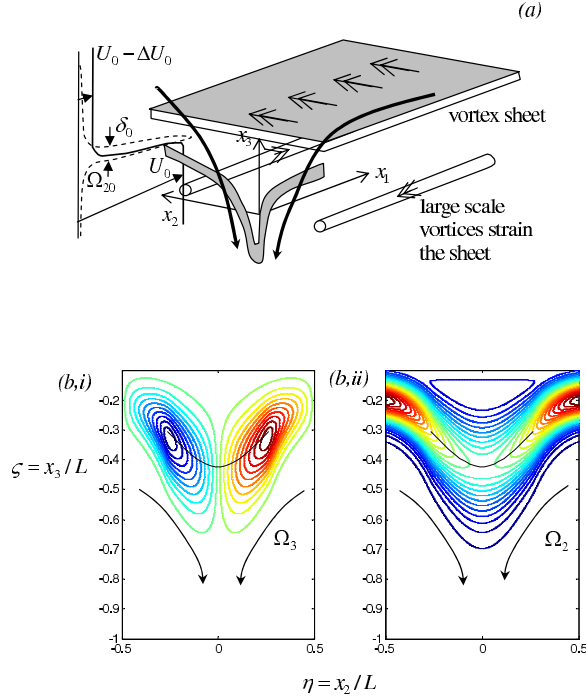


Fig. 2. (a) Schematic showing the engulfment of a sharp interface with a weak vortex sheet by a non-uniform straining flow generated by strong vortices. (b) Numerical solutions for contours of (i) Ω_3 , (ii) Ω_2 to the linearised vorticity equation (13) are presented which illustrate the straining and the diffusion of vorticity which limits the strength of Ω_3 . Here $\delta_0/L = 0.1$, $\beta = 2$.

the turbulent region are large compared to the velocity jump ΔU_1 across the interface.

Initially ($t = 0$) the sheared interface near $x_3 = x_3(0)$ has thickness δ_0 . In our model calculation, the initial cross-stream vorticity has a gaussian form,

$$\Omega_2(t = 0) = \Omega_{20} \exp(-x_3^2/2\delta_0^2), \quad \Omega_{20} = \Delta U_1/\delta_0\sqrt{2\pi}, \quad (10)$$

where ΔU_1 is the jump across the interface, which is expressed in terms of local dimensionless coordinates, corresponding to the velocity profile being an error function. The essential feature of the distortion and entrainment of the interface is a non-uniform straining flow generated by vortical pairs; in this approximate model, we consider a non-uniform straining incompressible flow described by

$$\mathbf{u} = \left(0, -\Sigma^{(-)}x_2(1 - \beta x_2^2/L^2), \Sigma^{(-)}(x_3 - L)(1 - 3\beta x_2^2/L^2)\right), \quad (11)$$

where β is a constant and a measure of the non-uniformity of the straining field. The intensity of turbulence is $u_0 \sim \Sigma^{(-)}L$. The distortion of a material sheet, representing the initial position of the vortex sheet, initially located at $x_3 = x_{3I}(t=0) (< L)$ by the flow field (9), is expressed in non-dimensional coordinates $\eta = x_2/L$, $\zeta = (x_3 - L)/L$, and time as $\tau = \Sigma^{(-)}t$.

We are interested in the entrained vortex sheet in the centre of the straining flow where $\eta \ll 1$. Here a point initially at (η_0, ζ_0) is advected to

$$\eta(\tau) \approx \eta_0 \exp(-\Sigma^{(-)}\tau), \quad \zeta(\tau) \approx \zeta_0 \exp\left(\Sigma^{(-)}\tau + \frac{3}{2}\Sigma^{(-)}\beta\eta_0^2(e^{-2\tau} - 1)\right). \quad (12)$$

Thus the shape of the interface as it deforms is a parabola whose curvature at the position of maximum penetration ($\eta_0 = 0$) $d^2\zeta/d\eta^2|_{\eta=0} = 3\beta\Sigma^{(-)}(e^{2\tau} - 1)$, increases rapidly. The vorticity field in the deformed interface Ω satisfies the linear vorticity equation

$$\frac{\partial\Omega}{\partial t} + (\mathbf{u} \cdot \nabla)\Omega = (\Omega \cdot \nabla)\mathbf{u} + \nu \left(\frac{\partial^2}{\partial x_2^2} + \frac{\partial^2}{\partial x_3^2} \right) \Omega. \quad (13)$$

The vortical dynamics are initially dominated by inviscid stretching/compression and later by viscous effects. For time $\tau \ll 1$, since the local Reynolds number is large, *i.e.* $Re = \Delta U_0 \delta_0 / \nu \gg 1$, inviscid dynamics prevail with

$$\frac{d\Omega_2}{d\tau} = -\Omega_2,$$

or

$$\Omega_2(\eta, \zeta, \tau) = \Omega_{20} \exp\left(-\frac{(\zeta \exp(-\Sigma^{(-)}\tau - \Sigma^{(-)}\frac{3}{2}\beta\eta^2(1 - e^{2\tau})) - \zeta_I)^2}{2\delta_0^2} - \tau\right), \quad (14)$$

so that the maximum spanwise vorticity in the vortex sheet decreases as

$$\Omega_{2max}/\Omega_{20} = \zeta_I/\zeta, \quad \zeta_I = (x_{3I} - L)/L, \quad (15)$$

due to the vortex lines being compressed (see Fig. 2(b,i)). At the same time, the vortex lines of the interface are being rotated generating a normal or x_3 -component of vorticity. Along the centreline of the deforming sheet, where $\eta = 0$, the interface is pinched, and combining (11) and (13) shows that, when viscous diffusion is small,

$$\frac{d\Omega_3}{d\tau} \approx \Omega_3 - 6\beta\eta\zeta\Omega_2. \quad (16)$$

Transforming η , ζ into Lagrangian coordinates, the approximate solution to (16), $\Omega_3(\eta \ll 1) \sim -6\beta\eta\zeta\Omega_2(\eta, \zeta, \tau)\sinh\tau$, where Ω_2 is given by (14). Thus the normal component of vorticity is rapidly amplified in the deformed parabolic interface with positive and negative signs for Ω_3 . The maximum

value of Ω_3 quickly becomes comparable to the undisturbed spanwise vorticity $\beta\Omega_{20}$, while Ω_2 decreases rapidly (see Fig. 2(b,ii))

In the asymptotic stage of the development and close to the centreline, where $3\beta(e^{2\tau} - 1)/2L \sim 1/\delta_0$ or $\tau \sim \log(L/\delta_0\beta)$, the interface is engulfed and the two branches of the interface come together. Enhanced diffusion serves to decrease Ω_3 . There is ultimately a balance for Ω_3 between advection in the η -direction/ ζ -direction, stretching in the ζ -direction and viscous diffusion in the η -direction so that

$$\zeta \frac{\partial \Omega_3}{\partial \zeta} - \eta \frac{\partial \Omega_3}{\partial \eta} = \Omega_3 + \frac{\nu}{\Sigma^{(-)}} \frac{\partial^2 \Omega_3}{\partial \eta^2}. \quad (17)$$

The similarity solution to (17), is

$$\frac{\Omega_3}{\Omega_{3max}} = -\frac{\hat{\eta}}{(\pi/2)^{1/2}} \exp\left(-\frac{1}{2}\hat{\eta}^2\right), \quad (18)$$

where $\hat{\eta} = \eta/\delta(t)$, $\delta(t)^2 = \nu/\Sigma^{(-)} + (\delta_1^2 - \nu/\Sigma^{(-)})(\zeta_1/\zeta)^2$ and $\Omega_{3max}\delta(t)\zeta = const$, where $\delta = \delta_1$ when $\zeta = \zeta_1$ (see [11], [12]). Thus the asymptotic thickness of the layer $\delta \rightarrow \sqrt{\nu/\Sigma^{(-)}}$ due to the balance between straining and diffusion (see [11], [12], [13]). The effect of cross-stream diffusion of vorticity is to reduce Ω_{3max} as ζ increases. For an initially thick interface ($\delta_0 \gg \sqrt{\nu/\Sigma^{(-)}}$), the interface thickness is rapidly reduced by straining but the decrease in the maximum vorticity is negligible. For an initially thin interface ($\delta_0 \ll \sqrt{\nu/\Sigma^{(-)}}$) straining increases the interface thickness and the maximum vorticity decreases rapidly. Thus the peak vorticity in the entrained interface $|\Omega_{3max}|$ is comparable to that at the interface.

The amplification of the vorticity component Ω_3 induces a jet parallel to the streamwise direction that lies between the distorted interfaces. For an initially thick interface, $\Omega_{3max} \sim \pm\beta\Omega_{20}$, the volume flux of the jet is approximately constant in time and of order - $|\Omega_{3max}|\delta_0 L \sim -\Delta U_1 L$ (for the flow in Fig. 2). As the average location of the interface $\langle x_{3I} \rangle$ moves outwards as a result of the bounding entrainment velocity E_b , it follows that there is an integral contribution to the average Reynolds stress produced by the engulfing motion, which is of the same order as that produced by turbulence, namely $-E_b \Delta U_1$ (see [14], §3). Since the mean velocity in the turbulent region is sheared, it follows that Ω_3 is also distorted in the x_1 -direction so that a streamwise component Ω_1 of the interface vorticity is generated, which affects the entrainment velocity E_b .

3 Conclusions

Vortices impinging on a strong free shear layer distort the ambient vorticity field with the cross-stream component of vorticity increasing due to the kinematic blocking effect of the interface. Longitudinal vortices create a streamwise

flow perturbation which increases as the inverse of distance from the interface or locally a logarithmic flow profile. This provides an alternative mechanistic explanation for the occurrence of a logarithmic profiles near rigid walls suddenly introduced into turbulent flows. Compact vortices create a weaker, and more localised, flow perturbation decaying as the inverse of distance from the interface. The entrainment of a weak shear layer by longitudinal vortices generates a cusped vortex sheet. As a consequence of the rotation of the vortical elements, a streamwise jet is created and an associated Reynolds stress.

These linearised calculations provide physical insight into some of the complex processes which are occurring and as consistent with the generally observations. The next step is a more detailed comparison against computational models.

References

1. DAVEY, M. & HUNT, J.C.R. 2006 Critical layers in geophysical flows. *Mathematics Today*.
2. WESTERWEEL, J., PEDERSEN, J.M., FUKUSHIMA, C. & HUNT, J.C.R. 2005 Mechanics of the turbulent/non-turbulent interface of a jet. *Phys. Rev. Letters*. **95** (17), 174501.
3. BISSET, D.K., HUNT, J.C.R. & ROGERS, M.M. 2002 The turbulent/non-turbulent interface bounding a far wake. *J. Fluid Mech.* **451**, 383–410.
4. MATHEW, J. & BASU, A.J. 2002 Some characteristics of entrainment at a cylindrical turbulence boundary. *Phys. Fluids*. **14**, 2065–2072.
5. CORRSIN, S. & KISTLER, A. 1955 Free stream boundaries of turbulent flows. *Tech. Rep Nasa 1244*, Washington DC.
6. TOWNSEND, A.A. 1966 The mechanism of entrainment in free turbulent flows. *J. Fluid Mech.* **26**, 689–715.
7. FERNANDO, H.J.S. & HUNT, J.C.R. 1997 Turbulence, waves and mixing at shear-free density interfaces. Part I - Theoretical Model. *J Fluid Mech.*, 347, 197–234.
8. HUNT, J.C.R. & DURBIN, P.A. 1999 Perturbed vortical layers and shear sheltering. *Fluid Dyn. Res.* **24**, 375–404.
9. REYNOLDS, W.C. 1972 Large-scale instabilities of turbulent wakes. *J. Fluid Mech.* **54**, 481–488.
10. PEROT, B. & MOIN, P. 1995. Shear-free turbulent boundary layers. Part 1. Physical insights into near-wall turbulence. *J. Fluid Mech.* 295, 199227.
11. BAZANT, M.Z. & MOFFATT, H.K. 2005 Exact solutions of the Navier–Stokes equations having steady vortex structures. *J. Fluid Mech.*, **541**, 55–64.
12. HUNT, J.C.R. & EAMES, I. 2002 The disappearance of laminar and turbulent wakes in complex flows. *J. Fluid Mech.* **457**, 111–132.
13. HUNT, J.C.R., EAMES, I. & WESTERWEEL, J.C. 2006 Mechanics of inhomogeneous turbulence and interfacial layers. *J. Fluid Mech.* **554**, 499–232.
14. TURNER, J.S. 1986 Turbulent entrainment: the development of the entrainment assumption, and its application to geophysical flows. *J. Fluid Mech.* **173**, 431–471.